BAUET JOURNAL
Published by
Bangladesh Army University of Engineering & Technology (BAUET)
Journal Homepage: https://journal.bauet.ac.bd/
DOI: https://doi.org/10.59321/BAUETJ.V5I1.4

Reduction of Torque Ripple and Input Current Harmonics in Closed-Loop V/f Controlled Induction Motor Drives

Md. Mehedi Hasan[1*], G.K.M. Hasanuzzaman[2], Md. Rubel Basar[1]

[1]*Department of Electrical and Electronic Engineering, Bangladesh Army University of Engineering & Technology, Qadirabad, Natore-6431, Bangladesh*
[2]*Department of Electrical and Electronic Engineering, Rajshahi University of Engineering & Technology, Rajshahi-6204, Bangladesh*

Abstract: Induction motors are extensively employed across various industrial applications, making efficient control strategies vital for improving performance, reducing operational costs, and enhancing system reliability. This study presents the implementation of a closed-loop Voltage-to-Frequency (V/f) control strategy for three-phase induction motor drives, with a focus on minimizing torque ripple and reducing input current harmonics. A systematic controller design is employed to iteratively fine-tune system parameters for improving dynamic response. Particular emphasis is placed on the reduction of input current harmonics and torque ripple—two critical factors influencing power quality and motor longevity. The performance of the designed controller is test by rigorous simulation. Simulation results demonstrate that the proposed approach reduces total harmonic distortion (THD) of the input current from 22.27% to 1.32%, and minimizes torque ripple from 1.50% to 1.08%. These improvements confirm that the proposed V/f control strategy, when combined with appropriate filtering, significantly enhances motor performance and stability under dynamic load conditions.

Keywords: *Induction Motor Drives, V/F Control, Harmonics Reduction, Torque Ripple Reduction*

Introduction: Induction motors (IMs) are widely used across various industrial sectors due to their durability, low maintenance requirements, and cost-effectiveness. Among the available control strategies, the constant voltage-to-frequency (V/f) control method has become one of the most popular for variable-speed applications. In this technique, the speed of the three-phase IM is regulated by controlling both the amplitude and frequency of the voltage supplied through a three-phase Voltage Source Inverter (VSI), maintaining a constant V/f ratio to ensure stable motor flux and torque [1]. Fluctuations in terminal voltage are often observed when motor speed is regulated by adjusting the supply frequency while attempting to maintain a constant voltage-to-frequency (V/f) ratio. Despite these variations, maintaining a constant V/f ratio enables the motor to achieve consistent torque output, especially across changes in speed [2]. This is because the stator magnetic flux—crucial for torque production—is directly proportional to the applied voltage and inversely proportional to the supply frequency. Since the motor's developed torque is fundamentally dependent on the stator's magnetic field, preserving a constant V/f ratio ensures stable flux and torque across the entire operating speed range [3].

In alternating current (AC) systems, ideal operation involves sinusoidal voltage and current waveforms, where linear loads draw current proportionally to the applied voltage. However, non-linear loads—such as those found in motor drive systems—tend to draw current only during specific portions of the voltage cycle, typically near the voltage peaks. This non-uniform conduction introduces harmonic components into the current waveform, leading to degraded power quality, increased losses, and potential interference with other equipment [4]. To mitigate these issues, various harmonic reduction techniques have been developed, including multi-pulse converter topologies, passive and active filtering methods, space vector modulation (SVM), and randomized pulse-width modulation (RPWM) schemes [5]. These methods aim to suppress harmonics, improve waveform quality, and enhance the overall performance and efficiency of motor drive systems. Torque ripple in electric machines primarily originates from cogging torque, magnetic field interactions, and mechanical imperfections such as rotor eccentricity [6]. In low-power induction motor drives (IMDs) employing V/f control, insufficient system damping can result in oscillations in the current waveform, as demonstrated in [7]. Although a Dynamic Current Compensator was introduced to suppress these oscillations, its effectiveness relied on the assumption of an ideal sinusoidal voltage source [8]. Other studies have explored alternative control models—such as a speed estimation approach for wind turbine emulation—which showed promise but were constrained to low-speed operation scenarios [9]. A hybrid pulse-width modulation (PWM) strategy was proposed in [10] to minimize torque pulsations with minimal current ripple; however, its capability to suppress higher-order harmonics remained limited. Meanwhile, Direct Torque Control (DTC) has been effectively applied to Permanent Magnet Synchronous Motors (PMSMs), offering high efficiency and rapid dynamic response, yet it remains challenged by significant torque ripple under low-speed operating conditions [11].

Article history:
Received 17 June 2025
Received in revised form: 27 August 2025
Accepted 23 September 2025
Available online 15 December 2025

Corresponding author details: Md. Mehedi Hasan
E-mail address: aurid1154637@gmail.com
Tel: +8801738204312

Variable switching frequency PWM techniques have been explored to reduce acoustic noise in induction motor drives; however, they often introduce unpredictable total harmonic distortion (THD) and increase switching losses, compromising overall efficiency [12]. To address torque ripple across varying speeds, advanced bus-clamping PWM schemes have shown effectiveness in maintaining smoother torque profiles [13]. Similarly, voltage source inverter (VSI)-fed drives have demonstrated reductions in both torque ripple and settling time, though their applicability is often limited to specific power levels [14]. Multilevel inverter (MLI)-based induction voltage-controlled IMD (IVCIMD) architectures have achieved low input current THD, yet at the expense of higher switching losses and reduced dynamic response [15]. In contrast, non-iterative Selective Harmonic Elimination (SHE) techniques have proven effective for medium-power variable-frequency applications, offering precise harmonic mitigation without iterative computation overhead [16]. A dynamic voltage restorer (DVR) approach utilizing a transistor-clamped H-bridge inverter has also been introduced to improve dynamic performance under power quality disturbances, successfully maintaining motor speed within acceptable limits [17].

For cost-sensitive applications, Arduino-based V/f control implementations offer a simplified and economical solution, though they typically lack real-time dynamic feedback capabilities required for adaptive control [18]. Finally, Space Vector PWM (SVPWM) has been recognized for improving both THD and speed response; however, its effectiveness has been validated primarily at high-speed operation levels (e.g., 1440 rpm), leaving performance at lower speeds less explored [19]. Despite of numerus study in open literature, the performance of existing controller in minimizing torque ripple and input current harmonics is limited. Therefore, this work proposes a closed-loop V/f-controlled induction motor drive system aimed at minimizing torque ripple and input current harmonics.

System Overview: This study proposes a closed-loop V/f-controlled induction motor drive system designed to improve power quality by reducing input current harmonics and torque ripple. The overall system architecture is depicted in Fig. 1. As it can be seen from Fig. 1, the designed process begins with a 6-pulse rectifier, which transforms AC voltage from the grid into unsmoothed DC voltage due to the presence of power electronic equipment. To address this issue, a DC link filter is employed to minimize voltage oscillations. The smoothed DC voltage is then fed into a 2-level, 3-phase inverter, where gate pulses for the IGBTs are generated using Sinusoidal Pulse Width Modulation (SPWM) technique. The SPWM pulses are created by comparing a controller output with a carrier signal. This controller operates as a closed-loop Voltage/frequency (V/f) controller.

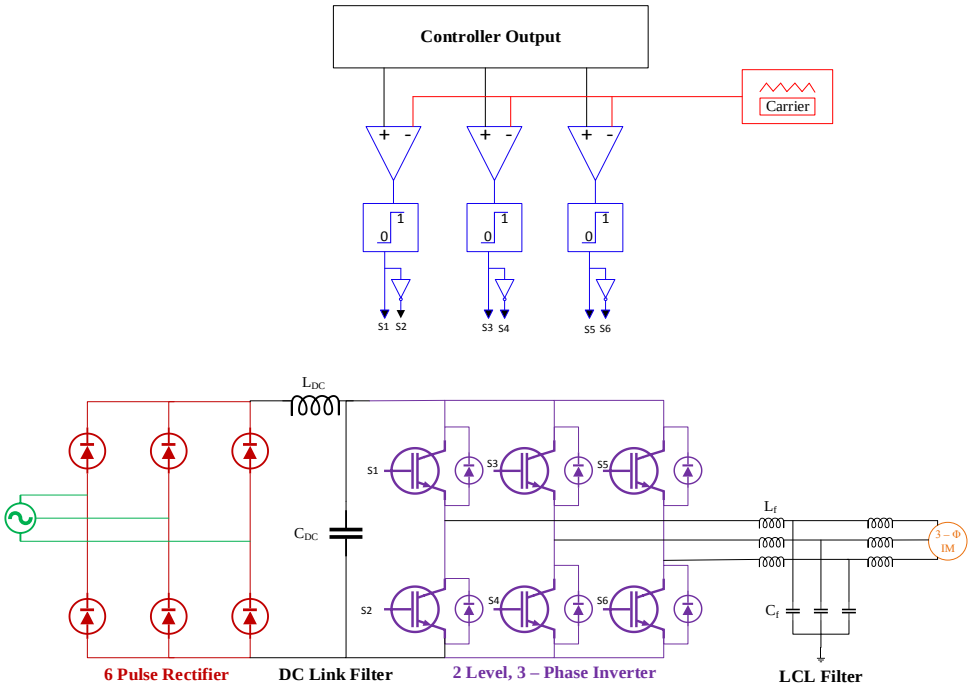

Fig. 1: System overview of closed-loop V/f-controlled induction motor drive system.

The switching frequency for the inverter is set at 10,000 Hz, significantly higher than the grid frequency of 50 Hz. Subsequently, the AC output from the inverter is connected to a 3-phase induction motor operating at 50 Hz and 415 Volts. V/f control methods are widely utilized in traditional industries to mitigate high input current harmonics and torque ripple. Consequently, this thesis aims to significantly reduce input current harmonics and torque ripple while operating with a high switching frequency relative to the grid frequency.

Table 1. Specifications of the IMD

Parameter List	Symbol	Value	Unit
Line-to-line Voltage	V_{LL}	415	V
Frequency	f	50.0	Hz
Stator Resistance	R_S	596.8	$m\Omega$
Stator Inductance	L_S	349.5	μH
Rotor Resistance	R_r	625.8	$m\Omega$
Rotor Inductance	L_r	5.47	mH
Mutual Inductance	L_m	35.4	mH
Moment of Inertia	J	0.05	$kg.m^{-2}$
Friction Coefficient	B	5.879	–
Number of Poles	P	2	Pairs

Control System Design: Fig. 2 illustrates the block diagram of the proposed closed-loop control system for a three-phase induction motor drive. The control strategy is based on maintaining a constant voltage-to-frequency (V/f) ratio using a PI (Proportional-Integral) controller. Closed-loop V/f control aims to maintain a constant V/f ratio to regulate the motor speed. Since the system involves high-frequency PWM (Pulse Width Modulation) control at 10 kHz, the control loop should be fast enough to respond to changes in the motor's speed. In the closed-loop V/f control of a three-phase induction motor, a PI controller is employed to maintain a constant V/f ratio with design parameters $K1 = 1/30$, $K2 = 2\pi$, and a frequency profile of $2\pi \times 50$. The proportional gain defines the immediate response to speed error, whereas the integral gain removes steady-state error.

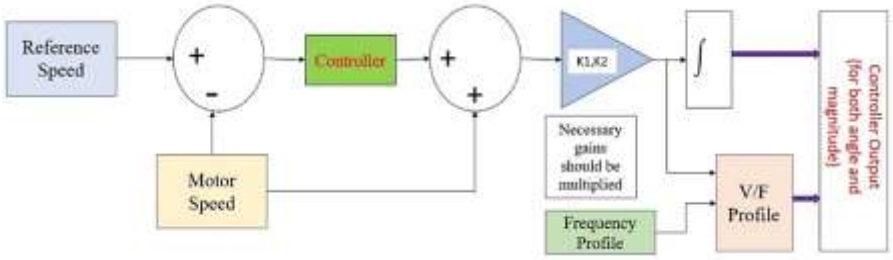

Fig. 2: Block diagram for proposed controller.

However, the exact values of P and I depend on various factors including the characteristics of motor, the dynamics of control system, and the desired performance specifications such as settling time, overshoot, and steady-state error tolerance as shown in Table 2. The proportional gain (P) defines the immediate response to speed error, whereas the integral gain (I) removes steady-state error. The tuning process starts with $P = 0$ and $I = 0$, P is gradually increased until the system exhibits stable behavior, followed by careful adjustment of I to eliminate residual error without inducing oscillations.

Table 2. Tuning Guidelines for PI Controller Parameters and Their Effects

Parameters	Rise Time	Settling Time	Overshoot	Steady-State Error
K_p	Decrease	Small Change	Increase	Decrease
K_i	Decrease	Increase	Increase	Eliminate

This PI controller provides an error signal. The proportional gain improves the speed of response by reducing the rise time and lowering the steady-state error, but it can slightly increase overshoot and has only a small effect on settling time. The integral gain also makes the response faster, yet it usually increases the settling time and overshoot because of its cumulative action. The main benefit of this PI controller is that it completely removes steady-state error, giving zero offset in the long run. Therefore, both proportional and integral gains must be tuned carefully to achieve a balance between fast response, low overshoot, and accurate steady-state performance. Then the PI controller response and motor speed will be further compared. Then the voltage amplitude and angle will be found by the designed controller, as it is shown in Fig. 3.

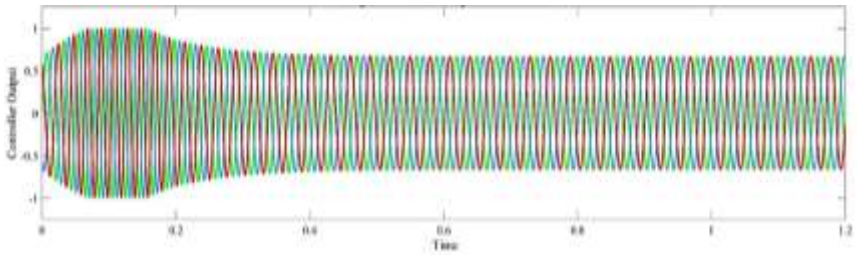

Fig. 3: Time-domain response of the controller output for the closed-loop V/f control system.

LCL Filter Design: An LCL filter is employed at the inverter output to suppress high-frequency switching harmonics and improve the quality of the delivered current. Compared to conventional L or LC filters, the LCL structure offers higher attenuation efficiency while requiring smaller component values. The filter is composed of an inverter-side inductor, a load-side inductor, and an intermediate shunt capacitor. This configuration effectively reduces switching ripple and produces a smoother sinusoidal waveform at the output. To mitigate resonance effects, damping is incorporated either through a small passive resistor or by adopting active damping methods within the control scheme. The integration of the LCL filter enhances power quality, reduces ripple content, and ensures stable operation of the proposed system. To complement the description of the LCL filter, the design procedure is summarized in Fig. 4. The figure outlines the key steps followed in determining the filter parameters, beginning with the identification of system requirements and proceeding through the selection of inductors, capacitor, and damping method.

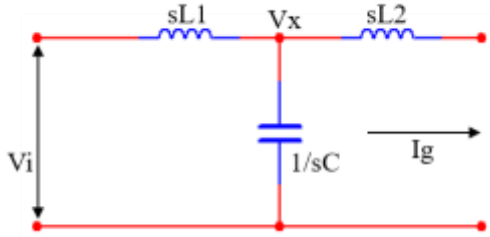

Fig. 4: LCL filter simplified diagram.

Applying KCL in Fig. 4, $\frac{V_i - V_x}{sL_1} = I_g + \frac{V_x}{1/sC}$ eq. 1

Also, $V_x = I_g \, sL_2$ eq. 2

Solving equation (1) and (2) we get, $\frac{I_g}{V_i} = \frac{1}{s^3 \, L_1 \, L_2 \, C + s(L_1 + L_2)}$ eq. 3

Assuming $L_1 + L_2 = L$ and $L_p = (L_1 L_2)/(L_1 + L_2)$,

We get, $\frac{I_g}{V_i} = \frac{1}{s \, L \, (1 + s^2 \, C L_p)}$ eq. 4

Also; $W_{res} = \frac{1}{\sqrt{C \, L_p}}$ eq. 5

Step-1: Selection of switching frequency (Let, $Fsw = 10 \, KHz$)

Step-2: Selection of resonant frequency ($Fres = Fsw / 10 = 1 \, KHz = 1000 \, Hz$)

Step-3: Finding the value of capacitance

Considering, Reactive power requirement = 5% of rated power

⇨ $Q = \frac{V^2}{(1/(2\pi f C)} = 5\%$ of S; eq. 6

⇨ $V^2 * 2\pi f C = 5\% \, of \, S$ eq. 7

⇨ $C = \frac{0.05 \, S}{V^2 (2\pi f)}$ eq. 8

Step-4: Tunning the value of inductor till L_{Max}

If, $I_g = \frac{KVA\ Rating/3}{Peak-to-peak\ Voltage}$ eq. 9

$L_{Max} = \frac{0.2 * V_{grid}}{2\pi * f_{grid} * I_g}$ eq. 10

DC Link Filter: The DC link filed as shown in Fig. 1 was tuned based on [15]:

Let, $V_{LL} = 0.612\ m_i\ (L-1)V_{DC}$ eq. 11

Where, V_{LL} = Line-to-line voltage, m_i = modulation index and L = dc link inductor and V_{DC} = dc voltage, L is used to boost up the dc voltage considering the filter and inverter losses.

If the grid voltage (415 V) and the IMD rated voltage (415 V) remain the same, the motor will operate inefficiently or may not run, making its use impractical. Therefore, the output of the rectifier must be boosted.

Assuming, if the DC voltage is boosted up from 415 V to 540 V, and modulation index is 200 (F_{SW} = 10000 Hz / f = 50 Hz), then equation (11) can be used to determine the required value of L. Subsequently, the DC-link capacitance C can be tuned appropriately to smooth the voltage ripple and maintain a steady DC voltage.

Result and Analysis: The performance of the proposed closed loop controller has been evaluated through comprehensive simulations in MATLAB SIMULINK environment and the simulated results have been presented in this section. The waveform presented in Fig. 5, demonstrate the dynamic behavior of the induction motor drive (IMD) during startup and transition to steady-state operation. Initially, the motor speed rises rapidly toward the reference value of 1000 rpm, accompanied by a sharp increase in torque and a substantial inrush current characterized by significant harmonic distortion. This behavior is typical during the acceleration phase. However, upon reaching the setpoint speed, the effectiveness of the filtering mechanism becomes evident as the stator current waveform stabilizes, and the harmonic content is significantly reduced. Simultaneously, the torque settles into a steady-state condition, indicating that the closed-loop V/f control strategy effectively manages transient disturbances and ensures smooth and stable operation of the motor drive system.

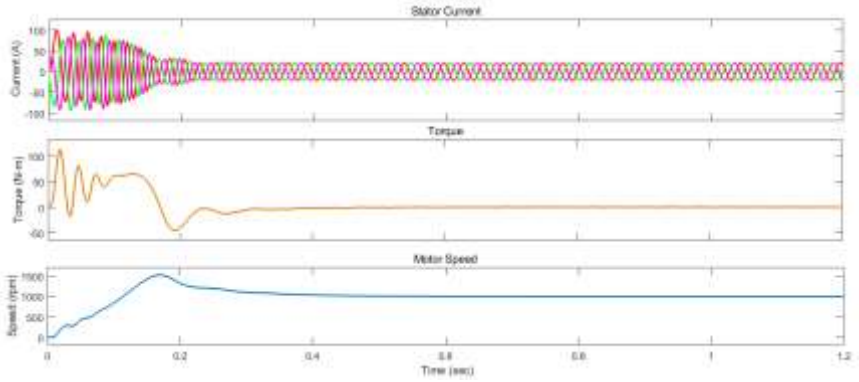

Fig. 5. Transient and steady-state response of the proposed closed-loop V/f-controlled induction motor drive.

During closed-loop operation, the controller consistently observes the feedback signals and dynamically adjusts the control inputs to the motor drive in real time as shown in Table 2. and Fig. 6. This adaptive feedback mechanism ensures that the motor maintains the desired speed and torque with high accuracy, even in the presence of external disturbances or varying load conditions. Throughout operation, the proposed controller continuously monitors the feedback signals from sensors and performs real-time error calculation and control signal adjustment. This persistent feedback mechanism ensures that the motor operates as closely as possible to the desired performance setpoints, even under varying operating conditions or external disturbances.

Table 2. Reference Speed Profile for Evaluating Closed-Loop Controller Performance

Time (s)	Applied Reference Speed (rpm)	Time (s)	Applied Reference Speed (rpm)
0.0	1200	3.0	200
0.5	1000	3.5	400
1.0	800	4.0	600
1.5	600	4.5	800
2.0	400	5.0	1000
2.5	200	5.5	1200

Fig. 6: Dynamic response for proposed closed loop IMD controller.

When there is a change in the load, the 3-phase induction motor dynamically adjusts its speed, torque, and current consumption to accommodate the new demand as show in the Fig. 7. This adaptive behavior ensures smooth and efficient operation, supported by features such as overload protection and the use of Variable Frequency Drives (VFDs), which enhance system robustness under significant load fluctuations.

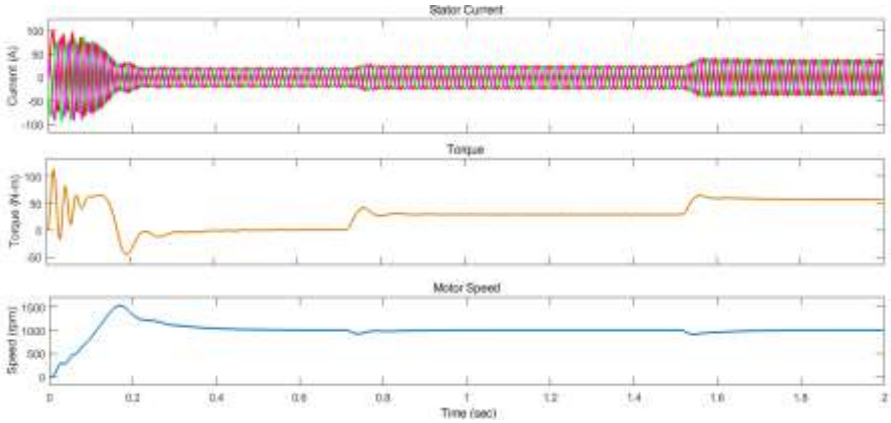

Fig. 7: System response to load perturbation at constant reference speed. A load of 28.3 $N.m$ is applied at 0.7 s and increased to 56.6 $N.m$ at 1.5 s, showing corresponding variations in stator current, torque, and motor speed.

As it can be seen from the Fig. 8 that changes in the reference speed of a 3-phase induction motor significantly affect the stator current waveform. These effects are governed by multiple factors, including the employed control strategy, dynamics characteristics of the motor, and the behavior of the associated power electronics. Typically, modifying the reference speed results in a corresponding change in the frequency of the voltage supplied to the motor, while directly impacts the frequency in the stator current waveform. Additionally, variations in reference speed affect the torque demand, thereby influencing the amplitude of the stator current as the motor adjusts to achieve the new operating condition. To evaluate the dynamic response of the proposed model, a step load equivalent to 50% of full load was applied at 0.5 seconds which caused the stator current to rise sharply, reaching a peak value of 55.54 A and an RMS value of 36.74 A. Then, the current subsequently stabilized by approximately 0.8 seconds. As illustrated in Fig. 9, the V/f control strategy dynamically adjusts both the supply voltage and frequency to maintain the desired torque-speed relationship when a load is applied. This adjustment consequently escalates motor current to generate the necessary torque. The proposed induction motor drive exhibits robust performance during a 50% load step applied at 0.5 s. The controller adjusts voltage and frequency in line with the load change, ensuring that current, torque, and speed remain stable without introducing oscillations or instability. This confirms the ability of the drive to deliver consistent and reliable operation under sudden load disturbances. The V/f control approach effectively balances torque, speed, voltage, and frequency thereby ensuring stable and efficient motor performance across diverse load scenarios.

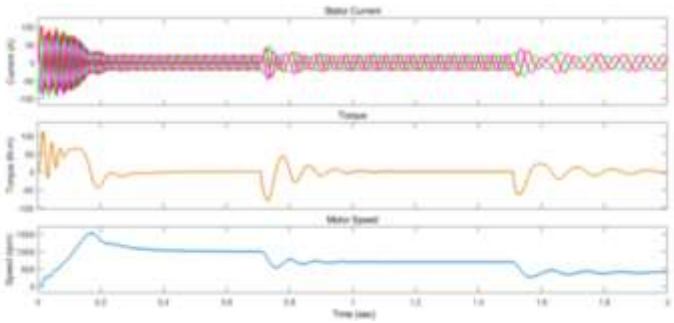

Fig. 8: Effect of reference speed variation on stator current, torque, and motor speed. The reference speed is reduced from 1000 rpm to 700 rpm at 0.7 s, and further to 700 rpm to 400 rpm at 1.5 s illustrating the system's dynamic response under step changes in speed demand.

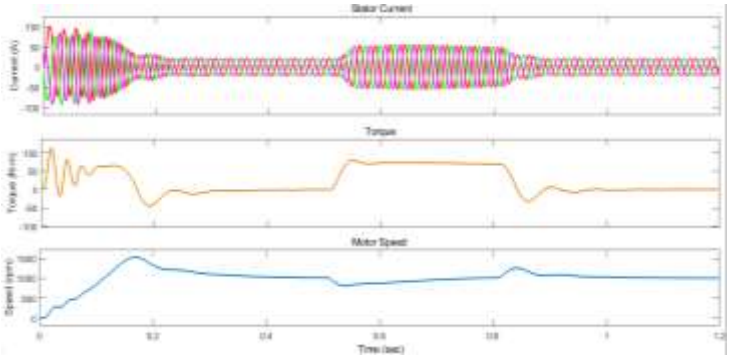

Fig. 9: Dynamic response of the proposed induction motor drive under a 50% load step at 0.5 s. The controller adjusts voltage and frequency proportionally to maintain torque, resulting in stabilized current, torque, and speed profiles.

A comparative summary of the system's performance under three different configurations is presented in Table 3 and Fig. 10 for three different cases. The results highlight the progressive improvement achieved in Total Harmonics Distortion (THD) and Torque Ripple (TR) through the inclusion of input filtering and subsequent fine-tuning of the controller parameters.

Table 3. Performance Comparison of Closed-Loop V/f Control Strategies in Terms of THD and TR

Case	Methodology	THD of Input Current	Torque Ripple
Case 01	V/f Closed-Loop Control without Filtering	22.27%	1.50%
Case 02	V/f Closed-Loop Control with Input Filtering	03.49%	1.10%
Case 03	V/f Control with Filtering and Controller Tuning (Trial & Error)	01.32%	1.08%

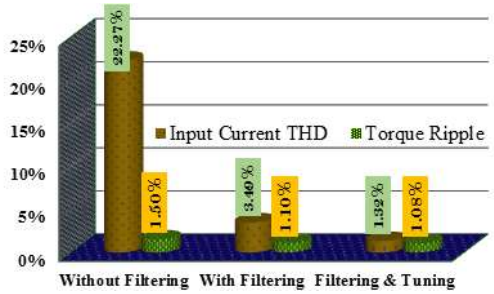

Fig. 10: Overall performance (THD & TR) comparison of proposed control system for three different cases

A comparative evaluation of the proposed system against existing techniques is presented in Table 4. The results show that the proposed method achieves substantial reductions in Total Harmonic Distortion (THD) and Torque Ripple (TR) compared to conventional approaches. These improvements arise from the use of optimized filtering and refined controller tuning, which

together enhance both power quality and dynamic performance. Overall, the comparison highlights the effectiveness of the proposed drive system in providing smoother torque and lower current distortion than existing techniques.

Table 4. Performance Comparison of existing models and proposed model in Terms of THD and TR.

Citation	Methodology	THD of Input Current	Torque Ripple
[15]	MLI based IVCIMD	03.10%	-
[19]	SVPWM Inverter (reduce THD) Using Constant V/F	20.14%	-
[5]	SPWM Inverter (Open Loop Configuration)	04.33%	1.24%
[5]	THPWM Inverter (Open Loop Configuration)	07.52%	1.51%
Proposed work	Closed Loop V/f Control based IMD with Filtering	01.32%	1.08%

Conclusion: This study demonstrates the proposed closed-loop V/f control strategy, combined with appropriate filtering, can significantly improve the performance of a three-phase induction motor drive. The total harmonic distortion (THD) of the input current was reduced to 1.32%, while torque ripple was minimized to 1.08%, indicating enhanced power quality and smoother motor operation. To achieve these results, an LCL filter was implemented between the inverter and the induction motor, along with a DC-link filter between the rectifier and inverter, effectively mitigating voltage oscillations and harmonic propagation. Despite these improvements, it is important to acknowledge that V/f control may exhibit limitations in dynamic performance, particularly under rapidly varying load conditions. Such scenarios can introduce fluctuations in motor speed, potentially impacting system stability. Therefore, while the proposed approach offers a cost-effective and efficient solution for steady-state applications, further enhancement—such as incorporating advanced control techniques—may be necessary for highly dynamic environments.

References:

[1] R. Bharti, M. Kumar, and B. M. Prasad, "V/f control of three phase induction motor, 2019 International Conference on Vision Towards Emerging Trends in Communication and Networking (ViTECoN), IEEE, March 30, 2019, pp. 1-4.
[2] S.V. Ustun, and M. Demirtas, Modeling and control of V/f controlled induction motor using genetic-ANFIS algorithm, Energy Convers. Manag, 50(3) (2009) 786-791.
[3] E. Saady, Gaber, El-Nobi A. Ibrahim, and M. Elbesealy, V/f control of three phase induction motor drive with different PWM techniques, Innovative Systems Design and Engineering, 4(14) (2013) 131-144.
[4] Priyadharshini, A., N. Devarajan, A.U. Saranya, and R. Anitt, Survey of harmonics in non-linear loads, Int. J. Recent Technol. Eng., 1(1) (2012) 92-97.
[5] S. P. Biswas, M. S. Anower, M. R. I. Sheikh, M. R Islam and K. M. Muttaqi, Investigation of the Impact of Different PWM Techniques on Rectifier-Inverter Fed Induction Motor Drive, Australasian Universities Power Engineering Conference, AUPEC 2020, Hobart, TAS, Australia, 29 November – 3 December, 2020, pp. 1-6.
[6] Torque ripple, eMetor, https://www.emetor.com/glossary/torque-ripple (accessed May 16, 2024).
[7] L. BEN-BRAHIM, Improvement of the stability of the V/f controlled induction motor drive systems, In IECON'98. Proceedings of 24th Annual Conference of the IEEE Industrial Electronics Society, August 31, 1998, vol. 2, pp. 859-864.
[8] J. Jung, G. Jeong, and B. Kwon, Stability Improvement of -Controlled Induction Motor Drive Systems by a Dynamic Current Compensator, IEEE transactions on industrial electronics, Castilla, 51(4) (2004) 930-933.
[9] R. Cardenas and R. Pena, Sensorless vector control of induction machines for variable-speed wind energy applications, IEEE transactions on energy conversion, 19(1) (2004) 196-205.
[10] K. Basu, J. S. S. Prasad, G. Narayanan, H. K. Krishnamurthy, and R. Ayyanar, Reduction of torque ripple in induction motor drives using an advanced hybrid PWM technique, IEEE Trans. Ind. Electron., 56(6) (2010) 2085–2091.
[11] Sivaprakasam Arumugam and Manigandan Thathan, Novel Switching Table for Direct Torque Controlled Permanent Magnet Synchronous Motors to Reduce Torque Ripple, Journal of Power Electronics, 13(6) (2013) 939-954.
[12] A. C. Binoj Kumar and G. Narayanan, Variable-switching frequency PWM technique for induction motor drive to spread acoustic noise spectrum with reduced current ripple. IEEE Transactions on Industry Applications, 52(5) (2016) 3927-3938.
[13] V. S. S. Pavan Kumar Hari and G. Narayanan, Theoretical and experimental evaluation of pulsating torque produced by induction motor drives controlled with advanced bus-clamping pulse width modulation, IEEE Transaction on Industrial Electronics, 63(3) (2016) 1404–1413.
[14] Chitra A et al., Performance Comparison of Multilevel Inverter Topologies for Closed Loop v/f Controlled Induction Motor Drive, 1st International Conference on Power Engineering, Computing and Control, Chennai, India, March 2-4, 2017, pp. 958-965.
[15] B. Singh and P. Kant, Multipulse AC–DC converter fed 15-level cascaded mli-based IVCIMD for medium-power application, IEEE Transactions on Industry Applications, 55(1) (2019) 858–868.
[16] P. Kant and B. Singh, Multiwinding Transformer Fed CHB Inverter with On-Line Switching Angle Calculation Based SHE Technique for Vector Controlled Induction Motor Drive, IEEE Transactions on Industry Applications, 56(3) (2020) 2807-2815.
[17] V. Khergade Anurag, R. J. Satputaley, V. B. Borghate, and B. V. S. Raghava, Harmonics reduction of adjustable speed drive using transistor clamped H-bridge inverter-based DVR with enhanced capacitor voltage balancing. IEEE Transactions on Industry Applications, 56(6) (2020) 6744-6755.
[18] A. R. Harsha et al. Arduino based V/f drive for a three-phase induction motor using single phase supply, 2020 International Conference on Smart Technologies in Computing, Electrical and Electronics (ICSTCEE), Oct. 09, 2020, 90-94.
[19] Sudaryanto Arif et al. Design and Implementation of SVPWM Inverter to Reduce Total Harmonic Distortion (THD) on Three Phase Induction Motor Speed Regulation Using Constant V/F, 3rd International Seminar on Research of Information Technology and Intelligent Systems (ISRITI), Dec. 10, 2020, 412-417.